Arctic Paleo-Oceanography in Late Cenozoic Time

Abstract. *Sediment cores from the Arctic Ocean yield significant faunal and lithologic evidence of alternating cold and milder periods for the last 6 million years. Although high-latitude continental glaciation commenced prior to 6 million years ago, the Arctic Ocean remained free of permanent pack ice up to approximately 0.7 million years ago, after which successive ice-covered and ice-free conditions existed.*

Faunal and sediment characteristics of more than 500 samples from 11 piston cores raised by Lamont-Doherty Geological Observatory were investigated. Of these, four from the Alpha Rise are discussed here (Table 1). [For results based on the remaining seven cores, see (*1*).]

The time interval represented by core T3-67-12 (Fig. 1) is thought to exceed 6 million years, thus providing the longest record of climatic and oceanographic history of the North Polar basin. Ages were estimated by interpolations and extrapolations based on radioisotope determinations (*2*) and close-interval faunal and lithologic cross correlation with neighboring cores. The neighboring cores were studied by Steuerwald *et al.* (*3*) and have an established paleomagnetic stratigraphy. If Steuerwald's correlations with Cox's (*4*) paleomagnetic time scale are correct, then the T3 cores described here represent 6 million years (Figs. 1 and 2).

Uranium series isotope ages indicate that in one core at the foot of the Alpha Rise (3437-m depth) sedimentation rates were of the order of about 2 mm per 1000 years during the last 150,000 years (*2*). Results of paleomagnetic studies (*3, 5*) support the radiochemically derived assessment of low sedimentation rates on the Alpha Rise and the Lomonosov Ridge. Age assignments of the various units discussed here are based on a small number of measurements and should therefore be considered provisional and subject to modification as additional radiometric and paleomagnetic determinations become available.

Ice-rafted debris throughout the cores

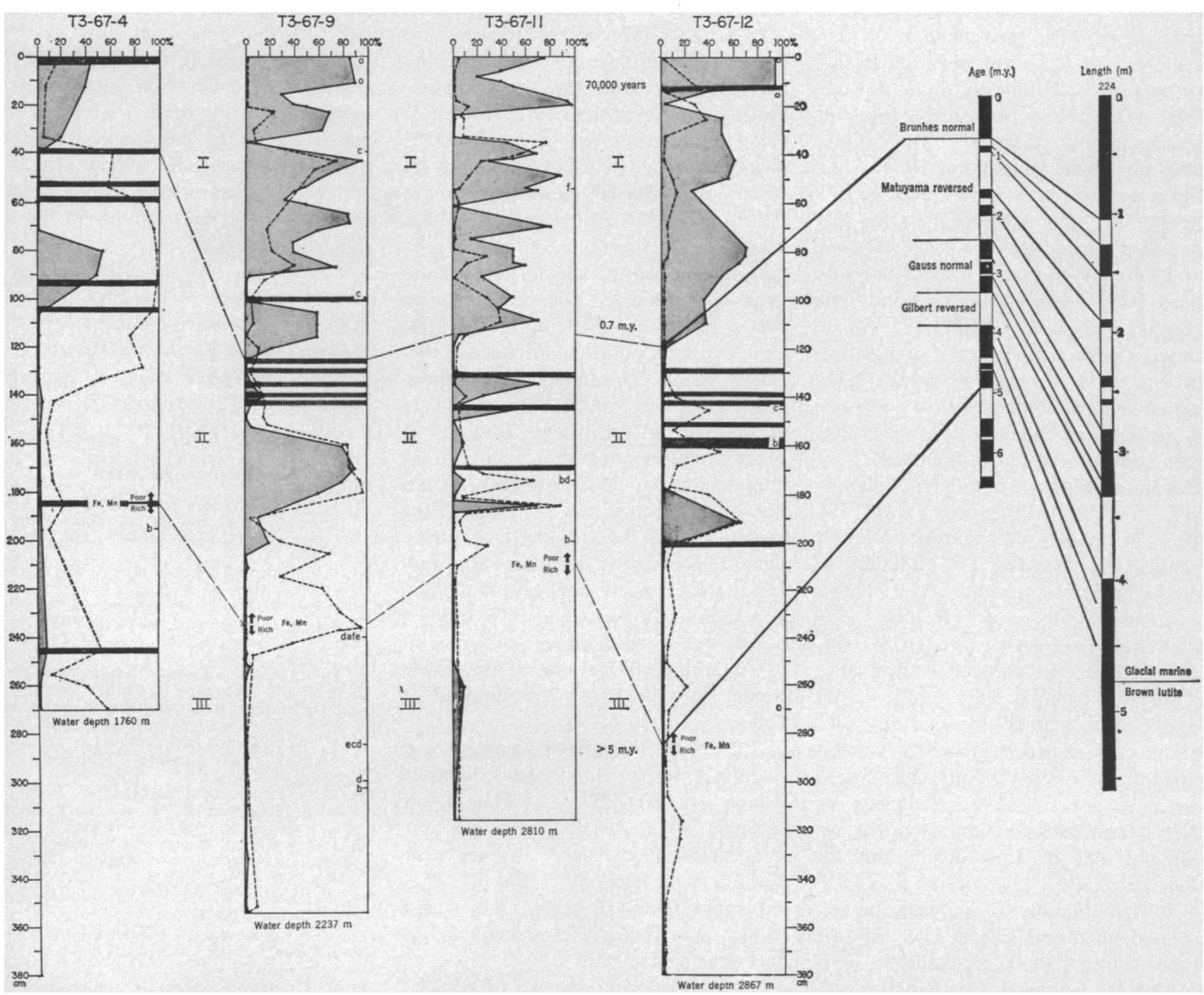

Fig. 1. Core depth in centimeters. Shaded areas represent volume percentages of microfauna. The dashed line shows the percentage of *Globigerina quinqueloba* complex out of the total planktonic population. Occurrence of low-latitude foraminifers is represented as follows: (*a*) *Globorotalia menardii* and *tumida*; (*b*) *Globorotalia scitula*; (*c*) *Globorotalia* sp.; (*d*) *Globigerinoides* sp.; (*e*) *Globigerinoides ruber*; and (*f*) *Sphaeroidinella dehiscens*. Circles represent pteropods. Dark, horizontal lines are horizons where benthonic foraminifers are in excess of 10 percent. On the right, the first column is the paleomagnetic time scale after Cox *et al.* (*4*); the second column is the core after Steuerwald *et al.* (*3*).

indicates that high-latitude glaciation commenced prior to 6 million years ago. Terrigenous sediments consist of clay- to pebble-sized clasts, all having a great range in degree of angularity. Sand-sized particles are principally composed of angular to subangular quartz, but well-rounded grains are present too. Granule- to pebble-sized clasts include limestones, shales, sandstones, and igneous and metamorphic fragments.

On the basis of faunal and sediment characteristics, three climatic units can be distinguished. The oldest, unit III (Fig. 1), was deposited between 6 and 5 million years ago; it consists of sediments that are rich in Mn and Fe oxides but that are poor in Foraminifera. Calcareous foraminifers are almost exclusively thick-shelled species, some of which are corroded. Embryonic thin-walled forms generally constitute 1 to 2 percent of the fauna in this unit but are much more abundant in units II and I. Arenaceous foraminifers (*Glomospira gordialis, Cyclammina pusilla,* and *Alveolophragmium subglobosum*) dominate the benthonic assemblages. Rates of sedimentation that were lower than present rates could account for the selective solution of the less resistant limy tests and the impoverished character of the calcareous fauna.

Unit II, deposited between approximately 5 and 0.7 million years ago, is poor in both Fe and Mn oxides and in Foraminifera, but it contains one Foraminifera-rich layer (Fig. 1). The predominant foraminifer in this layer is temperate-subarctic, euryhaline *Globigerina* sp. cf. *G. quinqueloba* (Fig. 3, b, d, and e) (*6*); this species occurs with sinistral *G. pachyderma* (Fig. 3, a, c, and f) throughout unit II (Fig. 1).

Minute, fragile, calcareous benthonic foraminifers (*Stetsonia horvathi, Sphaeroidina bulloides,* and *Bolivina* sp. A) periodically abound (Fig. 1) and constitute, together with other benthonic foraminifers, up to 88 percent of the fauna (Fig. 1). Concentration of thin-walled benthonic species suggests that the near absence of planktonic forms was not due to solution. In deep-sea sediments, benthonic foraminifers generally make up 1 to 5 percent of the total fauna. This major temporal change in the planktonic/benthonic ratio must have been induced by alteration in the environment; extreme conditions in the surface layers drastically reduced planktonic production.

Coarse ice-rafted detritus, including pebble-sized rock fragments and shallow

Table 1. Location, depth, and length of cores.

Core	Latitude (N)	Longitude (W)	Depth (m)	Length (cm)
T3-67-4	79°22.7′	174°46′	1760	272
T3-67-9	79°37.9′	172°07′	2237	356
T3-67-11	79°34.9′	172°30′	2810	250
T3-67-12	80°21.9′	173°33′	2867	374

water *Elphidium* spp., occur sporadically and are concentrated in zones dominated or followed by *Globigerina* sp., cf. *G. quinqueloba* (*6*). Possibly these layers were deposited intermittently, during short, mild episodes of intensified river runoff and ice-shelf melting. By basal freezing, lithic fragments and faunal remains were incorporated in shelf ice, which, after breaking, drifted across the Arctic. When thawing occurred, the entrapped debris was dropped to the sea floor.

Unit I was laid down in the last 0.7 million years during a time of conspicuous climatic fluctuations, as indicated by temporal variations in the faunal composition and in the faunal/mineral ratio (Fig. 1) (*1*). Foraminifera-rich and Foraminifera-poor beds alternate (Fig. 1). The beds that are rich in Foraminifera represent conditions similar to those prevailing today (permanent pack-ice cover) and contain cold water sinistral *Globigerina pachyderma* almost exclusively. However, *Globigerina* sp., cf. *G. quinqueloba* and *G. quinqueloba* s.s., attain high frequencies at the beginning and end of some of these cold periods (Fig. 1). This suggests temporary warming with subsequent increased glacial meltwater supply, followed by formation of surface water of low salinity to which eurythermal-temperate *Globigerina* sp. cf. *G. quinqueloba* and *G. quinqueloba* s.s., were able to adapt (*6*).

Fig. 2. Bathymetric map of the Arctic Ocean based on the Geological Map of the Arctic (1960). *T3,* Location of cores T3-67 at points 4, 9, 11, and 12; *PM,* cores with known paleomagnetic stratigraphy; *RI,* radioisotopically dated core. The open and closed circles show locations of previously studied cores (*1*).

In the Foraminifera-poor beds, the predominant cold water sinistral *Globigerina pachyderma* is accompanied by *Globigerina* sp., cf. *G. quinqueloba* and *G. quinqueloba* s.s.; occasionally other low-latitude foraminifers occur (Fig. 1) (*1*). A few pteropods are preserved, principally in core tops (Fig. 1).

Presence of ice-rafted detritus in the core bottoms indicates that high-latitude glaciation was under way prior to 6 million years ago. The progressive global cooling trend of the late Cenozoic eventually led to the growth and expansion of continental ice sheets. Removal of seawater and its storage on land in the form of glacial ice increased surface seawater salinities. Sinking of the dense saline water ensued, providing replenishment of oxygen to the bottom waters. Oxides of Fe and Mn were precipitated during this period. A change in the vertical structure of the Arctic water mass occurred at the boundary of units III and II about 5 million years ago. This alteration resulted in a decrease of Mn and Fe oxides (Fig. 1) concomitant with an increase in calcareous benthonic foraminiferal species and sporadic occurrence of coarse, ice-rafted rock fragments and of shallow water *Elphidium* spp. above the boundary. During the deposition of unit II, increased river runoff, iceberg and shelf-ice production, and consequent melting into the sea must have lowered surface water salinities and caused density stratification. At high latitudes, salinity is more important than temperature in determining water density; near the surface, slight reduction in salinity is sufficient to cause salinity stratification (*7*). Density stratification was sustained as long as fresh-water supply prevented sinking of the light surface water. The stability of water layers restricted vertical convection, and, consequently, nutrient levels and productivity were low; hence planktonic foraminifers are rare throughout most of this time interval. The absence of oxidized Mn and Fe in these sediments is further indication of reducing conditions at the water-sediment interface, inasmuch as reduced forms of Mn are more soluble in seawater than their oxidized counterparts.

It is assumed that the Arctic Ocean was free of permanent pack ice during the deposition of units II and III (*1*). The boundary of unit II and unit I corresponds to the last major polarity reversal of the earth's magnetic field (*3*), conveniently marking the Brunhes/Matuyama boundary. Continued global refrigeration accompanied by expansion of continental ice sheets and eustatic sea-level drop was coupled with continental uplift (*8*). These combined terrestrial effects gradually reduced the influx of warm Pacific and Atlantic water into the Arctic, converting it into an inland sea. Lowering of temperatures below a certain critical value permitted astronomical factors (essentially reduction in incoming solar energy) to trigger the initial major global glaciation and the ensuing glacial-interglacial oscillations that characterize the upper Pleistocene. It appears that the Brunhes/Matuyama boundary may coincide approximately with the onset of widespread continental glaciation at lower latitudes. My interpretation is in agreement with that of Emiliani and Geiss, Selli, and Berggren (*9*), who contend that at middle and low latitudes the preglacial Pleistocene was 1 to 1.5 times longer than the following ice epoch.

The low-latitude periodicity of climatic changes observed by Emiliani (*10*) and their coincidence with calculated past periodic fluctuations caused by iso-

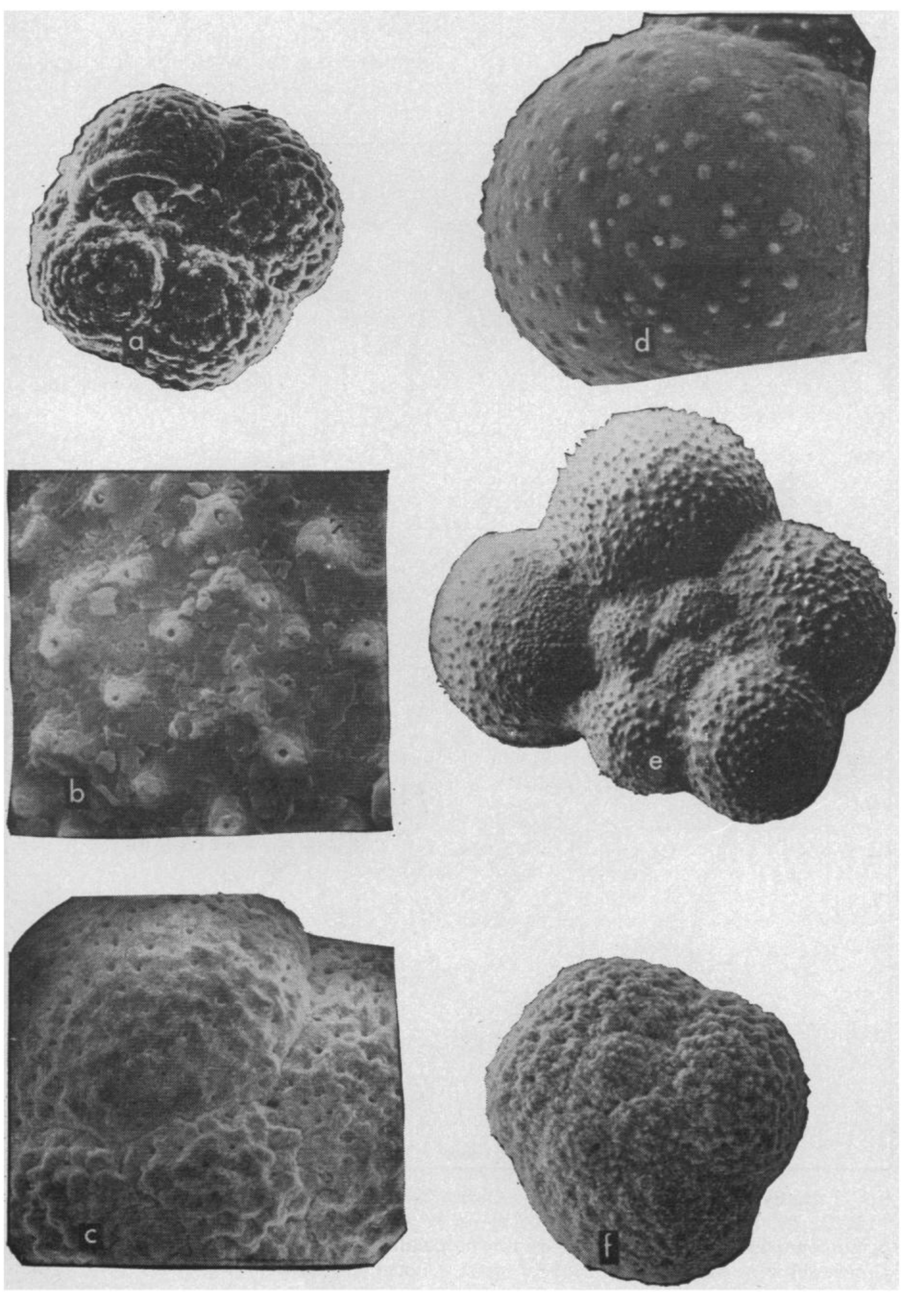

Fig. 3. (a) *Globigerina pachyderma* (dextral) (× 114); core T3-67-9, 220 cm. (b) *G. quinqueloba* (× 610), showing broken hollow spine bases; core T3-67-12, 192 cm. (c) *G. pachyderma* (sinistral) (× 160); core T3-67-11, 20 cm. (d) *G. quinqueloba* (× 320); core T3-67-11, 195 cm. (e) *G. quinqueloba* (× 120); core T3-67-9, 220 cm. (f) *G. pachyderma* (dextral) (× 160); core T3-67-11, 175 cm.

lation changes (*11*) is not matched by my findings in the Arctic. This discrepancy can be explained as follows. During prolonged warm periods, the heat supplied by solar radiation, required to increase surface water temperatures, also enhanced glacial melting. Consequently, as long as continental glaciers existed, seawater at high latitudes did not warm up to the same extent that it did at low latitudes. Alternately, it is conceivable that, owing to the extremely low rates of sedimentation in the investigated region of the Arctic, the resolution is much lower than that obtained by Emiliani in the Carribean (*12*). Emiliani (*10*) suggests the existence of "strong glaciations and warm interglacials" as well as "milder glacials and interglacials." It is quite possible that only during the long warm interglacials did the Arctic become free of permanent pack ice. The Foraminifera-poor beds were deposited in these intervals, whereas the Foraminifera-rich beds were laid down in "mild glacial" times. During the cold minima or "strong glaciations" of the last 0.7 million years, the Arctic surface must have been frozen all year round. Productivity must have been less than at present, and sediments deposited throughout these periods would be limited to clay-sized particles carried in suspension by deep currents. As a result, there would be practically no record of these intervals.

YVONNE HERMAN
Department of Geology, Washington State University, Pullman 99163, and U.S. Geological Survey, Menlo Park, California 94025

References and Notes

1. Y. Herman, *Nature* **201**, 386 (1964); *Palaeogeogr. Palaeoclimatol. Palaeoecol.* **5**, 251 (1969).
2. T. L. Ku and W. S. Broecker, *Progr. Oceanogr.* **4**, 105 (1967).
3. B. A. Steuerwald, D. L. Clark, J. A. Andrew, *Earth Planet. Sci. Lett.* **5**, 79 (1968).
4. A. Cox, R. R. Doell, G. B. Dalrymple, *Science* **144**, 1537 (1964).
5. T. I. Linkova, *The Present and Past of the Geomagnetic Field* (Nauka Press, Moscow, 1965), pp. 279–281; T. L. Ku, W. S. Broecker, N. Opdyke, *Earth Planet. Sci. Lett.* **4**, 1 (1968).
6. Y. Herman, C. Vergnaud Grazzini, C. Hooper, in preparation.
7. P. K. Weyl, *Meteorol. Monogr.* **8**(30), 37 (1968).
8. P. E. Damon, *ibid.*, p. 106; R. F. Flint, *Glacial and Pleistocene Geology* (Wiley, New York, 1957); W. Hamilton, *Meteorol. Monogr.* **8**(30), 128 (1968); W. F. Tanner, *ibid.*, p. 126.
9. C. Emiliani and J. Geiss, *Geol. Rundsch.* **46**, 576 (1967); R. Selli, *Progr. Oceanogr.* **4**, 67 (1967); W. A. Berggren, *G. Geol.* **35**(2), 291 (1968).
10. C. Emiliani, *J. Geol.* **74**, 109 (1966).
11. M. Milankovitch, *Handb. Geophys.* **9**, 593 (1938).
12. C. Emiliani, personal communication.
13. I thank K. Hunkins and C. Mathieu (Lamont-Doherty Geological Observatory) for collecting the cores; R. R. Capo (Lamont-Doherty Geological Observatory) for sampling and shipping the core samples; C. Hooper for able laboratory assistance; P. E. Rosenberg, D. M. Hopkins, C. Emiliani, Tj. H. van Andel, and J. W. Mills for critically reading the manuscript; and N. Schneiderman, W. A. Berggren, and D. Becker for the scanning electron micrographs (SEM) of the Foraminifera. Coring operations and curatorial services were supported by Lamont-Doherty Geological Observatory grants ONR .266-82, ONR (N 000 14-67-A-0108-0004), and NSF GA-10635. N. Schneiderman's SEM were taken with a Cambridge Mark II A instrument at the Central Electron Microscopy Laboratory, University of Illinois, W. A. Berggren's SEM were taken with a JEOLCO instrument at Woods Hole Oceanographic Institution, and D. Becker's SEM was taken with a Cambridge Mark II A instrument at Engis Western Corporation, Palo Alto.

3 February 1970; revised 2 June 1970

Hydrogen Bonding in Hydrochloric Acid Solutions

Abstract. *The radial distributions of atom pairs in water and in solutions of hydrochloric acid have been measured by x-ray diffraction. The near-neighbor water correlations are strongly affected by the ions. Part of the experimental distributions is attributed to new oxygen-to-oxygen distances, associated with the presence of excess protons, and these distances become shorter as the concentration of the acid increases.*

Theoretical activity, stemming, in part, from experiments relating to "anomalous water," has developed regarding shorter than normal oxygen-hydrogen-oxygen bond distances in water (*1*). The actuality of "anomalous water" (as a single-phase, pure material) has been challenged (*2*). Nonetheless, the structural calculations, as they relate to the symmetry and length of the O–H bonds and the magnitude of the O–O distances, may be of broader significance. Indeed, those parameters in crystalline materials have been a matter of interest for some years (*3*), and their possible role in solutions has been briefly considered (*4*). We therefore report preliminary results of an x-ray diffraction study of HCl solutions, which may be relevant in a consideration of O–H–O bonding.

A more or less direct reduction of the x-ray intensity scattered by a liquid specimen yields a pair distribution function, $4\pi r^2\rho(r)$. For a pure liquid $4\pi r^2\rho(r)\,dr$ would be the number of atom centers in a spherical shell of radius r and thickness dr, centered on an average atom. For a polyatomic material the function is the sum of partial functions, corresponding to each of the possible pair types, with each partial function weighted on the basis of the relative scattering power of that particular pair (*5*).

Figure 1 shows the $4\pi r^2\rho(r)$ functions for pure water and for 2*N*, 4*N*, and 6*N* HCl solutions at 25°C. The average density curves, $4\pi r^2\rho_0$, are also shown. An earlier x-ray study of an HCl solution (*6*) exists but, because of an insufficient range of $\sin\theta/\lambda$, it shows too little resolution in $\rho(r)$ to allow real comparison. In pure water, the most probable near-neighbor O–O distance is about 2.8 Å. As HCl is added, the corresponding peak broadens into a shape which is characteristic of an overlap at a 2*N* concentration and which does become resolved at higher concentrations. It is possible to fit that region of the pair density function with peaks centered at 2.75 and 3.20 Å for 2*N*, 2.68 and 3.25 Å for 4*N*, and 2.56 and 3.20 Å for 6*N* concentrations. A near absence of any pairs at the pure water O–H–O distance of 2.8 Å may be seen directly in the results for the 6*N* solution. An additional peak also develops at about 2.1 Å; because of its position and magnitude we believe it to be due to H–Cl pairs. The peak at 3.2 Å matches expectations for a well-defined O–Cl [or O–H–Cl (*7*)] interaction distance. X-

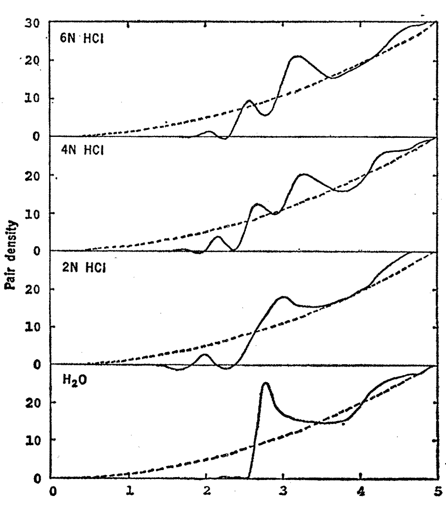

Fig. 1. Distribution of atom pairs in water and HCl solutions. (Solid lines) $4\pi r^2\rho(r)$; (dashed lines) $4\pi r^2\rho_0$.